JOURNAL OF MATERIALS SCIENCE 20 (1985) 3131 – 3140

Impact fracture behaviour of double-base gun propellants

R. C. WARREN
Weapons Systems Research Laboratory, Defence Research Centre Salisbury, GPO Box 2151, Adelaide, South Australia 5001, Australia

Impact fracture properties of three nitrocellulose–nitroglycerine gun propellants have been measured in a three-point bend mode at moderate impact rates with an instrumented drop-weight impact tester. Dynamic moduli and loss tangents were measured over the temperature range −100 to +120° C, and three transitions were identified. A transition at about −30° C was found to increase the low-temperature fracture toughness of the higher nitroglycerine content propellants. The fracture data were analysed in terms of plane stress and plane strain fracture modes using a simplified model. It was found that the fracture toughness in zones undergoing plastic deformation under plane stress conditions was approximately twice that in zones under plane strain conditions. The plastic zone radii were greater than 0.3 mm at 20° C, falling to about 0.1 mm at −45° C. Strain energy release rates were calculated from fracture load and modulus, and from fracture energy. Good agreement was obtained between the two methods.

1. Introduction

Gun propellant grains are subject to large impulsive stresses during the ignition cycle. Fracturing of grains under these circumstances causes an increase in burning surface, leading to variations in muzzle velocity or, in the worst case, to catastrophic failure of the gun. Gun propellants become more brittle at low temperatures, and some propellants are unusable below −40° C.

The fracture resistance of a grain is influenced both by the grain geometry and the inherent fracture toughness of the propellant. Gun propellant grains range in size from about 1 mm diameter and several millimetres long, up to 10 mm diameter and 30 mm long, with symmetrically spaced perforations in the axial direction. The thickness of the webs in the grains ranges from about 0.3 to 1 mm. For webs as thin as this, it is unlikely that fracture would occur under purely plane strain conditions. Consequently the standard tests of plane strain fracture toughness of materials may not be relevant to gun propellants, and some more appropriate test method may be required.

Large-calibre gun propellants are usually based on plasticized nitrocellulose (NC), with or without particulate fillers. The plasticizers can be energetic, e.g. nitroglycerine (NG), or non-energetic, e.g. dibutyl phthalate. Propellants containing principally NC and NG are known as double-base propellants. The only previously reported measurement of fracture toughness of a double-base propellant was a study by Kinloch and Gledhill [1, 2] of fracture properties of a rocket propellant containing NC plasticized with 42% NG and 2.8% dibutyl phthalate. The stress intensity factors were measured over the temperature range −60 to +20° C at very low strain rates using compact tension test specimens. These test conditions were appropriate for rocket propellants. Fracture occurred when the plastic zone at the notch tip reached a radius of approximately 1.3 mm. They also found that the fracture toughness at about −40° C was increased by the presence of a secondary transition in the propellant.

The behaviour of filled propellants is of major interest, but the added complication of

0022–2461/85 $03.00 + .12

matrix–filler interactions was considered to be too great for an initial study of impact properties. This paper describes a programme of work using an instrumented drop-weight tester to study the fracture properties of three double-base propellants. The aims of this work were to determine whether the secondary transitions in gun propellants cause significant changes in fracture energy under impact conditions, and whether plastic deformation under plane stress conditions is likely to play a significant part in fracture behaviour.

2. Theory

2.1. Critical stress intensity factors

The fracture behaviour of propellants is of interest mainly at low temperatures, where fracture occurs in a brittle mode. Under these conditions the propellant behaves as an elastic body, the strains are less than a few per cent, and the assumptions of linear elastic fracture mechanics apply.

The stress intensity factor K, which relates the magnitude of the stress intensity at the notch tip to the gross stress in the specimen σ, is given by

$$K = Y\sigma a^{1/2} \quad (1)$$

where a is the initial notch depth and Y is a geometrical factor which has been determined for several geometries [3]. Crack propagation will occur when K exceeds a critical value K_c, the critical stress intensity factor.

The strain energy release rate G_c is the energy per unit thickness required to advance the crack by unit distance. G_c is related to K_c by

$$K_c^2 = G_c E \quad \text{(plane stress)} \quad (2a)$$

$$K_c^2 = G_c E(1 - \nu^2) \quad \text{(plane strain)} \quad (2b)$$

where E is Young's modulus and ν is Poisson's ratio.

A method of calculating G_c directly from the measured fracture energy has been given by Brown [4] and by Marshall *et al.* [5]. For a notched bar undergoing three-point bending, G_c is related to the area w under the load–deflection curve by

$$w = G_c BD\phi + w_{KE} \quad (3)$$

where B is the specimen thickness and D is the width. ϕ is a geometrical factor related to the specimen compliance, values of which have been tabulated by Plati and Williams [6]. The fracture energy also includes a contribution from the gain in kinetic energy of the specimen, w_{KE}. Assuming that the transfer of kinetic energy is the same for all tests, an estimate of the size of the kinetic energy term can be obtained by plotting the fracture energy w against $BD\phi$. The slope of the curve gives G_c, and the intercept on the energy axis gives the kinetic energy contribution.

2.2. Effect of notch geometry

In notched specimen bars the value of K_c varies along the notch. Near the surface, at the ends of the notch, the stress field is plane stress and shear plastic deformation can occur with the dissipation of energy. At the centre of the notch, the stress field corresponds to plane strain and plastic deformation tends to be inhibited. Estimates of the magnitude of the plane stress and plane strain components of fracture can be obtained using the simplified model of fracture behaviour for low rate testing described by Parvin and Williams [7]. The method had been extended to impact conditions by Newmann and Williams [8].

The specimen can be considered as a sandwich of two outer layers of thickness r_{p_2} in plane stress, and an inner plane strain layer of thickness $B - 2r_{p_2}$. With these assumptions, the value of G_c obtained from a test is an average given by

$$BG_c = G_{c_1}(B - 2r_{p_2}) + G_{c_2}2r_{p_2} \quad (4)$$

where subscripts 1 and 2 refer to plane strain and plane stress respectively. Therefore

$$G_c = G_{c_1} + \frac{2r_{p_2}}{B}(G_{c_2} - G_{c_1}) \quad (5)$$

Parvin and Williams [7], and Kinloch and Gledhill [1, 2] analysed fracture in terms of K_c, with a plane strain component K_{c_1} and a plane stress component K_{c_2}. K_c was apportioned according to

$$K_c = K_{c_1} + \frac{2r_{p_2}}{B}(K_{c_2} - K_{c_1}) \quad (6)$$

However, substituting Equation 2 into Equation 5 gives

$$K_c^2 = K_{c_1}^2 + \frac{2r_{p_2}}{B}(K_{c_2}^2 - K_{c_1}^2) \quad (7)$$

Equations 6 and 7 are mutually incompatible.

The stress field at the crack tip is complicated, and it is not obvious how K_c should be apportioned between K_{c_1} and K_{c_2}. Yap *et al.* [9] have reviewed the available evidence and concluded that, while the difference between Equations 6 and 7 is not great, the energy partition is more appropriate, and so Equations 5 and 7 will be used here.

For cases where the plastic zone radius r_p is much less than the notch depth a,

$$r_p = \frac{EG_c}{2\pi\sigma_y^2} = \frac{1K_c^2}{2\pi\sigma_y^2} \quad (8)$$

where E is Young's modulus and σ_y is the uniaxial tensile yield stress. There are several possible values of G_c or K_c that have been used in Equation 8. If it is assumed that the zone size is affected only by the plastic deformation process, then K_{c_2} and G_{c_2} are appropriate. However, Yap *et al.* [9] consider that the zone size varies with sample thickness and that the measured values of K_c and G_c should be used to calculate the values of r_p which are substituted in Equations 5 or 7.

2.3. Measurement of modulus and yield stress

If values of E and σ_y can be determined, measurements of G_c for at least two thicknesses B can be used to set up simultaneous equations for G_{c_1} and G_{c_2}. However, it is necessary to measure Young's modulus and yield strength under the same conditions as the fracture properties.

It is suggested that values of σ_y and E can be obtained under impact conditions by testing unnotched specimens. A typical load–time curve for an unnotched bar of propellant is characterized by an initial linear section followed by a curved section as the material yields. A straight-line fit can be obtained for the linear part, and a second order equation can be fitted to the curved part. The load at yield P, is determined from the point of intersection of the lines of best fit. A similar procedure has been used to determine the yield from load–deflection curves of other polymers [10]. For three-point bending over a span S, the stress is a maximum on the bottom face of the specimen, and so when the specimen yields the yield stress is given by

$$\sigma_y = \frac{3PS}{2BD^2} \quad (9)$$

The ratio of deflection at yield d to load at yield is the compliance of the specimen C_0, which is related to the modulus E by

$$C_0 = \frac{d}{P} = \frac{S^3}{4EBD^3} \quad (10)$$

Hence

$$E = \frac{S^3P}{4dBD^3} \quad (11)$$

3. Experimental procedure

3.1. Materials

The propellant ingredients were mixed with processing solvents in a 1 kg Winkworth incorporator at 50° C for 4 h and then extruded at 50° C through a square die with 10 mm sides. The resulting extrudate was stoved at 50° C for three weeks to remove the solvents. Test specimens were milled from the dried extrudate. The size of the specimens was limited by the difficulty of completely removing solvent from large sections. The compositions of the propellants were 20:79:1, 35:64:1 and 45:54:1, where the figures are percentages of NG, NC and stabilizer respectively.

3.2. Dynamic mechanical measurements

Dynamic Young's modulus and $\tan\delta$ were measured using a Polymer Laboratories dynamic mechanical thermal analyser in the single-cantilever mode. The temperature range from -100 to $+120$° C was scanned at 5° C min^{-1}, with test frequencies of 0.33, 3, and 30 Hz. The specimens were 6mm × 2 mm in section, with a test span of 7.9 mm.

3.3. Impact testing

The impact testing was carried out on a Dynatup Model 8200 instrumented drop-weight tester linked to an ETI 300 microprocessor-controlled data acquisition system (Effects Technology Inc., Santa Barbara, USA). The specimens were supported on anvils 36 mm apart and tested in the three-point bend mode at an impact velocity of 0.55 m sec^{-1}. Load and energy were recorded as functions of time. Four to six tests were conducted at each test condition and the results were averaged.

Modulus and yield stress were determined using unnotched bars machined to size 6 mm × 6 mm × 45 mm. K_c was determined using bars machined to sizes 6 mm × 2 mm × 45 mm and 6 mm × 2 mm × 45 mm, with a

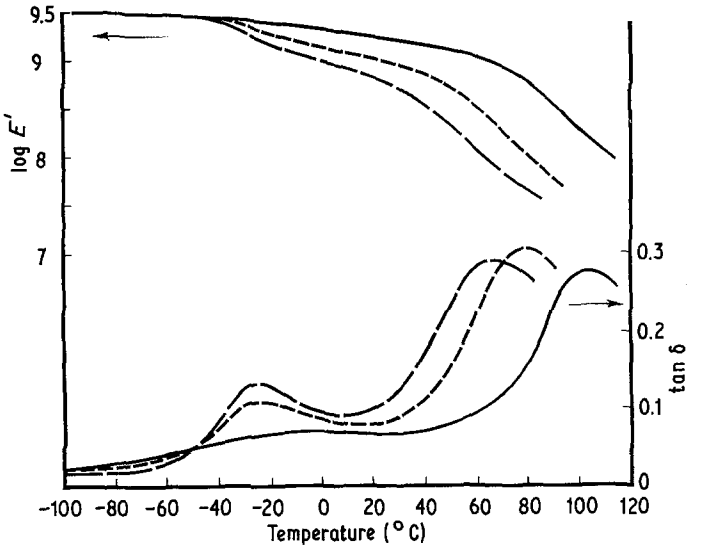

Figure 1 Young's moduli and mechanical loss factors of double-base propellants (E' in MPa); — 20% NG, – – – 35% NG, — — 45% NG.

tolerance of 0.1 mm. Sharp notches nominally 1.5 mm deep were produced by slowly forcing razor blades into specimens precooled in dry ice. The actual notch depth was measured after fracture using a travelling microscope.

Test temperatures were -60, -45, -30, -15, 0 and $+20°$ C for all propellants, and several intermediate temperatures for some propellants. For testing at sub-ambient temperatures, the specimens were conditioned at the test temperature in a conditioning cabinet for 30 min, then removed and tested within 10 sec.

4. Results and discussion

4.1. Dynamic mechanical analysis

Curves of Young's modulus and tan δ measured at 30 Hz over the temperature range -100 to $+120°$ C are shown in Fig. 1. A relatively large transition, designated α, occurred above about 70° C, and a smaller transition, designated β, occurred in the temperature range -30 to 0° C. The tan δ curves for the 20% NG propellant are above the curves for the other propellants at temperatures below $-50°$ C, and this is due to the presence of a third transition, designated γ. This transition has been observed previously in pure NC and in poorly plasticized propellants at about $-80°$ C, and it is progressively replaced by the β transition as the NG content is raised [11].

Measurements made at frequencies of 0.33, 3, and 30 Hz indicated that the temperature of peak tan δ of the β transition increased by 10° C for a one hundred-fold increase in frequency.

4.2. Impact testing

Typical load against time traces for notched specimens are given in Fig. 2. The oscillations in the trace are due to small vibrations in the load cell, and not to variations in the load on the specimen, which are much smaller [12]. For specimens of the same span and width, the amplitude of the oscillation is approximately proportional to the specimen mass, and consequently its thickness. The slope of the load–time curve is also proportional to the specimen thickness, so the ratio of the oscillation amplitude to the fracture load is the same for both specimen thicknesses.

The specimen load can be approximated by a straight line of best fit, and the fracture load was determined from the value of the smoothed curve at the time of fracture as indicated in Fig. 2. The factors affecting the vibrations were analysed, and it was concluded that reducing impact velocity was the only way of minimizing inertial effects. In the present case the effective strain rate was 15 sec^{-1}.

The values of modulus E and yield stress σ_y, are given in Table I. Critical stress intensity factors for the 2 and 6 mm thick specimens are given in Table II. The propellant containing 45% NG did not fail in a brittle mode at 20° C, and none of the unnotched specimens showed any yielding at $-60°$ C. The values in parentheses are unbiased estimates of the population standard deviations of the quantities. The standard deviations of E were about 5% and the standard deviations of σ_y and K_c were generally in the range 5% to 10%.

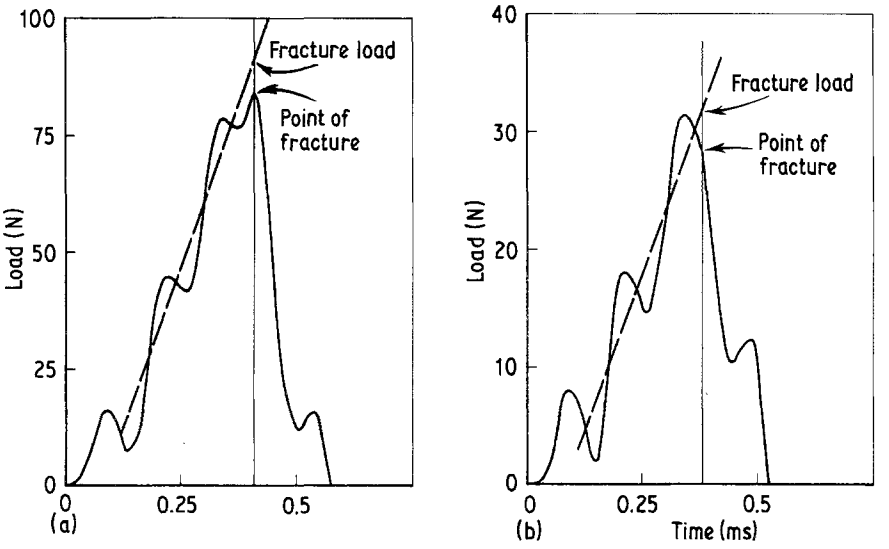

Figure 2 Load against time traces for bars of 20% NG propellant at $-30°$ C. (a) 6 mm, (b) 2 mm thick specimens.

The moduli of all propellants decreased rapidly over the temperature range -60 to $+20°$ C, and the values were lower for the more highly plasticized propellants, as would be expected. The stress intensity factors and yield stresses were less dependent on temperature. The yield stresses doubled as the temperature ranged between $+20$ and $-45°$ C, but K_c showed the opposite trend with the values at $-45°$ C being approximately half the values at 20° C. The values of K_c of the 20% NG propellant at low temperatures were about 50% higher than for the 45% NG propellant.

These results can be compared to those obtained by Kinloch and Gledhill [1, 2] on rocket propellants tested at the very low rate of 10^{-5} sec^{-1}. In that case measurements were made on compact tension test pieces 10 and 50 mm thick, over the temperature range -60 to

TABLE I Mechanical properties of propellants

NG (%)	Temperature (° C)	Modulus (GPa)*	Yield stress (Pa × 10^{-7})
20	+20	3.19(0.11)	7.15(0.63)
	0	4.10(0.14)	8.20(0.83)
	−15	4.81(0.43)	8.45(0.18)
	−30	5.99(0.21)	11.25(0.65)
	−45	7.00(0.47)	11.63(0.18)
	−60	7.16(0.34)	†
35	+20	1.95(0.11)	4.73(0.23)
	0	2.57(0.13)	5.83(0.13)
	−15	3.63(0.10)	8.43(0.25)
	−22	–	–
	−30	4.90(0.26)	10.00(0.63)
	−45	6.52(0.25)	10.03(0.45)
	−60	7.16(0.38)	†
45	+20	–	–
	0	1.96(0.08)	4.70(0.33)
	−15	2.60(0.14)	5.77(0.40)
	−30	3.68(0.23)	7.95(0.48)
	−37	–	–
	−45	5.82(0.26)	9.00(1.2)
	−60	6.85(0.37)	†

*Standard deviations in brackets.
†No yield at $-60°$ C.

TABLE II Critical stress intensity factors

NG (%)	Temperature (° C)	Critical stress intensity factor K_c (MN $m^{3/2}$)*	
		6 mm	2 mm
20	+20	1.57(0.05)	1.95(0.26)
	0	1.61(0.07)	1.56(0.10)
	−15	1.45(0.08)	1.49(0.10)
	−30	1.46(0.08)	1.45(0.12)
	−45	1.40(0.27)	1.44(0.09)
	−60	1.36(0.15)	1.53(0.10)
35	+20	2.12(0.22)	2.77(0.31)
	0	1.59(0.07)	1.86(0.21)
	−15	1.46(0.14)	1.61(0.10)
	−22	1.40(0.11)	1.65(0.10)
	−30	1.12(0.03)	1.25(0.05)
	−45	1.20(0.05)	1.37(0.12)
	−60	1.15(0.09)	1.25(0.10)
45	+20	–	–
	0	1.53(0.05)	1.91(0.15)
	−15	1.25(0.12)	1.56(0.08)
	−30	1.38(0.08)	1.53(0.08)
	−37	1.06(0.03)	1.14(0.11)
	−45	0.95(0.04)	1.13(0.09)
	−60	1.01(0.08)	1.11(0.15)

*Standard deviations in brackets.

TABLE III Fracture parameters calculated from r_p derived from $K^*_{c_2}$

NG (%)	Temperature (° C)	K_{c_1} (MN m$^{3/2}$)	K_{c_2} (MN m$^{3/2}$)	G_{c_1} (J m^{-2})	G_{c_2} (J m^{-2})	r_p (mm)
20	+20	1.34(0.21)	3.00(0.38)	565(175)	2800(720)	0.28(0.09)
	0	–	–	–	–	–
	−15	1.43(0.13)	2.00(0.85)	425(85)	840(710)	0.09(0.08)
	−30	–	–	–	–	–
	−45	1.38(0.41)	2.21(2.72)	270(165)	700(1700)	0.06(0.14)
	−60	1.27(0.25)	–	–	–	–
35	+20	1.70(0.48)	3.13(0.25)	1490(845)	5010(850)	0.69(0.13)
	0	1.44(0.18)	2.57(0.32)	800(205)	2560(660)	0.31(0.08)
	−15	1.38(0.23)	2.57(0.49)	525(175)	1810(690)	0.15(0.06)
	−22	1.26(0.20)	2.94(0.31)	365(115)	2030(490)	0.16(0.04)
	−30	1.05(0.06)	2.44(0.21)	225 (25)	1220(220)	0.09(0.02)
	−45	1.11(0.11)	2.66(0.37)	190 (40)	1090(300)	0.11(0.03)
	−60	1.10(0.15)	–	170 (50)	–	–
45	+20	–	–	–	–	–
	0	1.30(0.14)	2.48(0.18)	860(190)	3130(465)	0.44(0.09)
	−15	1.06(0.22)	2.41(0.19)	435(180)	2240(370)	0.28(0.06)
	−30	1.30(0.14)	2.45(0.31)	460(100)	1630(425)	0.15(0.04)
	−37	1.02(0.08)	2.00(0.47)	225 (30)	845(405)	0.09(0.05)
	−45	0.85(0.09)	2.39(0.28)	120 (25)	980(240)	0.11(0.04)
	−60	0.96(0.15)	–	135 (45)	–	–

*Standard deviations in brackets.

+20° C. The values of K_c were similar at −60° C but they decreased with increasing temperature, which is opposite to the trend in the present work. The yield stresses were less by at least a factor of four. These differences could be due to the large difference in testing rates.

4.3. Effect of plastic deformation

At temperatures above −30° C, the values of K_c determined from the 2 mm thick specimens were higher than those determined from the 6 mm thick specimens, and the differences were found to be significant at the 1% confidence level using the Student's t test. The only exceptions are the results for the 20% NG propellant at 0 and −30° C, which may be affected by experimental scatter. These observations indicate that the measured fracture toughness is dependent on the geometry of the test specimen, and to obtain an estimate of the magnitude of this effect the fracture results were analysed using the plane strain–plain stress fracture model described by Equation 7.

The value of the plastic zone size r_p to be used in Equation 7 can be calculated from either the plane stress fracture toughness K_{c_2}, or from the values of the measured K_c for the particular specimen thicknesses [9]. No shear lips were observed on the fracture surfaces, so it was not possible to directly determine which method of calculation was most appropriate. Hence, it was decided to calculate the effects of plastic deformation using both methods and to compare the results.

Assuming that the plastic zone size is determined by the value of K_{c_2}, Equations 7 and 8 were used to calculate K_{c_1}, K_{c_2}, G_{c_1}, G_{c_2}, and r_p. The values are given in Table III, together with the calculated standard deviations in parentheses. Standard deviations of the derived quantities were estimated using the following approximate relationship [13]:

$$var(F) = \left(\frac{\partial F}{\partial a}\right)^2 var(a) + \left(\frac{\partial F}{\partial b}\right)^2 var(b) + \ldots \quad (12)$$

where *var* is the variance and F is a function of measured quantities a, b, ...

The values of the standard deviations of K_c were generally in the range 10 to 20%, while the values for G_c and r_p were up to 30%. From Table III it can be seen that K_{c_1} showed a slow decrease of up to 30% with decreasing temperatures in all propellants. K_{c_2} was about twice K_{c_1}, but it showed only a slight decrease with decreasing temperature. Both G_{c_1} and G_{c_2} show a steep decrease with decreasing temperature.

The alternative method of calculating plastic

TABLE IV Fracture parameters calculated from r_p derived from K^*_c

NG (%)	Temperature (° C)	K_{c_1} (MN m$^{-3/2}$)	K_{c_2} (MN m$^{-3/2}$)	G_{c_1} (J m^{-2})	G_{c_2} (J m^{-2})	r_p (mm)
20	+20	1.45(0.08)	4.06(0.82)	655(75)	5180(2110)	0.12(0.04)
	0	–	–	–	–	–
	−15	1.43(0.12)	2.35(2.24)	425(85)	1150(2190)	0.05(0.01)
	−30	–	–	–	–	–
	−45	1.38(0.39)	2.95(7.85)	275(155)	1240(6620)	0.02(0.01)
	−60	1.29(0.20)	–	235(70)	–	–
35	+20	1.93(0.25)	3.31(0.43)	1910(515)	5620(1640)	0.55(0.13)
	0	1.49(0.10)	3.14(0.71)	870(130)	3830(1740)	0.16(0.04)
	−15	1.40(0.19)	3.59(1.48)	540(145)	3550(2940)	0.06(0.01)
	−22	1.31(0.14)	4.63(0.98)	405 (90)	5020(2130)	0.05(0.01)
	−30	1.07(0.04)	4.25(0.75)	235 (20)	3680(1321)	0.02(0.01)
	−45	1.14(0.07)	4.59(1.52)	200 (25)	3220(1760)	0.03(0.01)
	−60	1.11(0.13)	–	172 (40)	–	–
45	+20	–	–	–	–	–
	0	1.41(0.07)	2.88(0.32)	1015(105)	4240 (980)	0.26(0.06)
	−15	1.15(0.14)	3.29(0.52)	510(130)	4170(1350)	0.12(0.02)
	−30	1.32(0.11)	3.44(0.94)	475 (85)	3230(1770)	0.06(0.01)
	−37	1.03(0.06)	3.11(1.69)	220 (25)	2040(2210)	0.03(0.01)
	−45	0.89(0.05)	4.50(1.01)	135 (15)	3490(1560)	0.03(0.01)
	−60	0.97(0.12)	–	135 (35)	–	–

*Standard deviations in brackets.

zone size from the measured value of K_c for each specimen thickness gave the values of the fracture parameters and plastic zone size listed in Table IV. The values of K_{c_1} and G_{c_1} are similar to the values obtained from the first method at low temperatures, but are marginally higher at high temperatures. The calculated errors of K_{c_2} of the 20% NG propellant below 20° C are so large that the K_{c_2} values are meaningless, and the fracture effectively occurs in plane strain. The standard deviations of K_{c_2} are approximately twice as large as from the first method, and the standard deviations of G_{c_2} are correspondingly higher. K_{c_2} increases with decreasing temperature, which is opposite to the trend in the first method. Above −30° C the plastic zone sizes were 50 to 70% less.

The divergence of the values calculated by the two methods is disturbing, and it is not apparent from these experiments which method is more soundly based. However, the smaller calculated errors for the first method indicate that it may be useful as a semi-empirical procedure for estimating the magnitude of effect of plane stress deformation in the fracture of propellant grains.

Despite the uncertainty over the exact values of the size of the plastic deformation effects it is apparent that, compared with propellant grain web thicknesses of 0.5 to 1 mm, the calculated zone of deformation is significant above about −30° C for 35 and 45% NG propellants. For 20% NG propellants the plastic zones size is significant above about 0° C.

This suggests that at high temperatures the fracture in propellant grains occurs largely in plane stress, but as the plastic zone radius shrinks with decreasing temperature the fracture becomes more brittle under plain strain conditions. This factor may contribute to the increase in brittleness observed in some propellants below about −40° C.

Kinloch and Gledhill [1, 2] found that the zone of plastic deformation in plane stress had a constant radius of 1.3 mm at fracture over the temperature range studied. The larger plastic zone radius in this case may be due to a lower value of yield stress at the lower testing rate.

4.4. Effect of secondary transitions on fracture properties

Secondary transitions provide a mechanism for dissipating energy, and so would be expected to increase the strain energy release rate G_c. Boyer [14] has reviewed some of the evidence relating impact strength and secondary transitions, and Hartmann and Lee [15] have demonstrated such a relationship in polycarbonate. While there is no generally accepted physical explanation for a

TABLE V Strain energy release rates

NG (%)	Temperature (° C)	G_c (J m^{-2})	
		6 mm	2 mm
20	+20	770(55)	1190(320)
	0	630(60)	595 (80)
	−15	435(60)	460 (75)
	−30	355(40)	350 (60)
	−45	280(110)	295 (40)
	−60	260(60)	325 (45)
35	+20	2300(495)	3935(910)
	0	985(100)	1345(310)
	−15	590(115)	715 (90)
	−22	455(75)	630 (80)
	−30	255(20)	320 (30)
	−45	220(20)	290 (50)
	−60	185(30)	220 (35)
45	+20	–	–
	0	1195(90)	1860(300)
	−15	600(120)	935(110)
	−30	515(70)	635 (80)
	−37	245(20)	280 (55)
	−45	155(15)	220 (35)
	−60	150(25)	180 (50)

relationship, the same authors [16] suggested that the stress waves caused by the impact could be attenuated by the loss mechanism responsible for the transition processes.

For a comparison of G_c and tan δ to be valid, both quantities have to be calculated at the same effective frequency. The impact event involves a wide range of frequencies, but Hartmann and Lee [15] have analysed the frequency spectrum of a Charpy type test, and found that the first minimum occurs at a value of $\omega D = 8$, where ω is the circular frequency and D is the test duration. In the present case the duration of the impacts at −30° C is approximately 0.3 msec, so the most important frequencies would be below about 3.6 kHz. The tan δ curves were obtained at 30 Hz, a factor of about a hundred less than the highest frequencies in the impact event. The dynamic mechanical measurements in Section 4.1 indicated that a hundred-fold increase in frequency corresponded to an increase in temperature of 10° C, so the tan δ curves would have to shifted to higher temperature by about 10° C to match the G_c curves.

The uncertainty in the calculated values of G_{c_2} precludes their use for comparison with mechanical loss factors. Instead, the values of G_c from the 2 and 6 mm thick specimens were used. The values are listed in Table V, are illustrated in Figs. 3 to 5, together with the corresponding

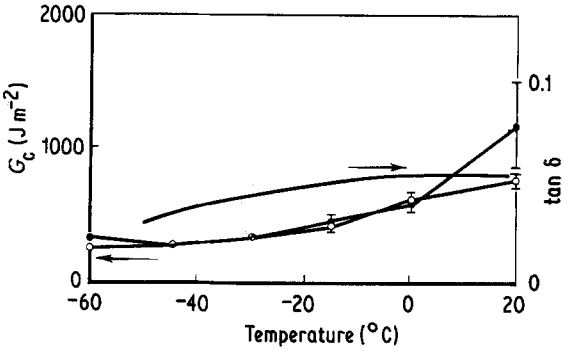

Figure 3 Comparison of G_c from 2 mm (●) and 6 mm (○) thick specimens with tan δ for the 20% NG propellant; bars = standard deviation.

tan δ curves shifted to higher temperatures by 10° C.

Propellants containing 35 and 45% NG show an initial rapid decrease in G_c with decreasing temperature from 20° C, but the rate of decrease tends to level off at about −20° C. At about −20° C to −30° C these propellants show a step to lower G_c at low temperatures. The 20% NG propellant behaves differently, showing only a gradual decrease in G_c with decreasing temperature, and below −35° C, G_c is greater than for the more highly plasticized propellants.

It can be seen from Figs. 3 to 5 that the G_c and the tan δ curves for each propellant have

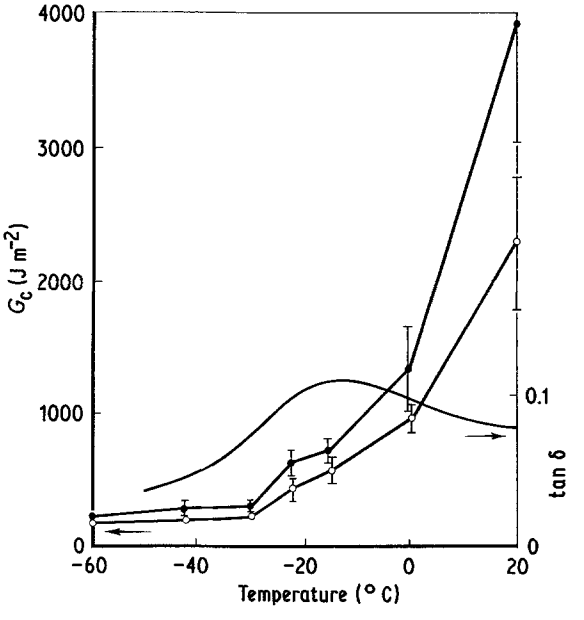

Figure 4 Comparison of G_c from 2 mm (●) and 6 mm (○) thick specimens with tan δ for the 35% NG propellant; bars = standard deviation.

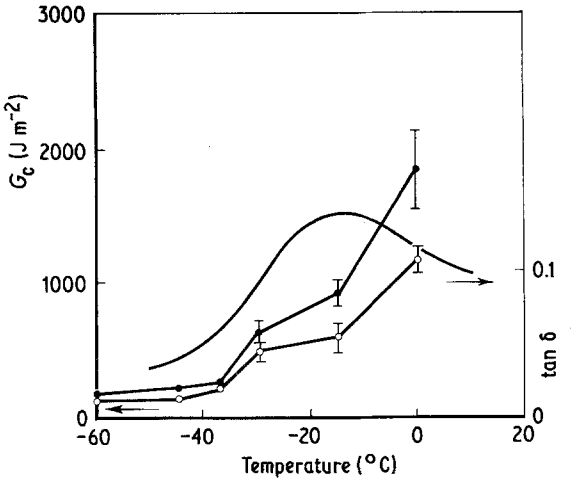

Figure 5 Comparison of G_c from 2 mm (●) and 6 mm (○) thick specimens with tan δ for the 45% NG propellent; bars = standard deviation.

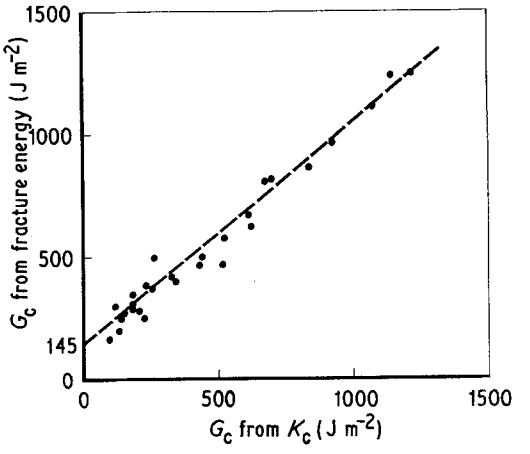

Figure 6 Comparison of values of G_c calculated from fracture energy and fracture load; —— straight line of best fit.

qualitative similarities, with the steps in the G_c curves corresponding to the β transition peaks. This result is a strong indication that the β transition can have a significant effect on fracture energy.

Kinloch and Gledhill [1] observed a peak in G_{c_2} at about $-40°$ C which was associated with a peak in mechanical loss due to the β transition.

4.5. Calculations of G_c

The availability of values of fracture loads and energies for each test allows a comparison of values of G_c calculated from K_c and E using Equation 2, and from the fracture energy using Equation 3. Values of G_c from both methods are given in Table IV and values below 1500 J m^{-2} are plotted in Fig. 6 (kinetic energy effects were ignored initially). Higher values are mostly from the 2 mm thick specimens, which were affected by plastic yielding. It can be seen that the overall agreement is very good, but at low energies Equation 3 consistently gives higher values. The points in Fig. 6 are well fitted with a straight line of slope 0.837 and an intercept on the vertical axis of 145 J m^{-2}, with a correlation coefficient of 0.987.

The neglect of the kinetic energy term in

TABLE VI Strain energy release rates

Temperature (° C)	NG (%)	From fracture energy (J m^{-2})		K_c^2/E (J m^{-2})	
		6 mm	2 mm	6 mm	2 mm
+20	20	873	1167	803	1228
	35	2698	4540	2482	3992
	45	–	–	–	–
0	20	682	634	721	609
	35	1020	1300	1059	1390
	45	1291	1984	1306	1920
−15	20	523	555	505	518
	35	725	865	707	780
	45	630	920	670	960
−30	20	455	475	406	390
	35	307	555	275	319
	45	524	730	603	713
−45	20	349	435	228	286
	35	338	429	252	305
	45	259	365	168	227
−60	20	402	444	228	286
	35	312	333	179	194
	45	222	359	132	159

Equation 3 is probably responsible for the higher values of G_c calculated from this equation. It was observed that the broken test pieces bounced to a height of about 100 mm, and the kinetic energy calculated from this bounce height increases G_c by about $100\,J\,m^{-2}$. While the calculation is very approximate, this value is of the same order as the measured excess G_c of $145\,J\,m^{-2}$. Marshall *et al.* [5] suggested calculating the kinetic energy term by plotting the measured energy w against $BD\phi$, and measuring the intercept on the energy axis. However, in the present case the appropriate measurements were not made.

5. Conclusions

The fracture toughnesses of three double-base gun propellants consisting of nitrocellulose plasticized with 20, 35 and 45% nitroglycerine have been determined at an impact velocity of $0.55\,mm\,sec^{-1}$. The calculated values of fracture toughness depended on specimen thickness, indicating that fracture occurs in a mixed plane stress–plane strain mode. Analysis of the data in terms of a two phase model of a plane strain region sandwiched between two plane stress regions indicated that in almost all cases the fracture toughness was at least twice as high in the plane stress zone.

The size of the zone of plastic deformation in plane stress at 20° C appears to be a significant fraction of the web thickness of many gun propellant grains, indicating that the fracture energies of these grains may be enhanced by the energy dissipated by plastic deformation. The plastic zone size decreases with decreasing temperature, which causes the grains to become more brittle at low temperatures as fracture progressively occurs with a larger plane strain component.

The secondary transition occurring at about −30° C was found to significantly increase fracture toughness of the higher nitroglycerine content propellants at low temperatures. Values of G_c were calculated from measured K_c and moduli, and also from the measured fracture energy. The overall agreement between the methods was good.

Unfilled propellants only have been studied here. Futher work is being undertaken to investigate the effects of particle-filler interactions on fracture of filled propellants.

References

1. A. J. KINLOCH and R. A. GLEDHILL, International Conference on Nitrocellulose Characterisation, Propellants Explosives and Rocket Motor Establishment, Waltham Abbey, UK, May 1980.
2. R. A. GLEDHILL, A. J. KINLOCH, *Propell. Explos.* **4** (1979) 73.
3. J. E. SRAWLEY, "Fracture", Vol. 4, edited by H. Liebowitz (Academic, New York, 1969) p. 63.
4. H. R. BROWN, *J. Mater. Sci.* **8** (1973) 941.
5. G. P. MARSHALL, J. G. WILLIAMS and C. E. TURNER, *ibid.* **8** (1973) 949.
6. E. PLATI and J. G. WILLIAMS, *Polym. Eng. Sci.* **15** (1975) 470.
7. M. PARVIN and J. G. WILLIAMS, *Int. J. Fract.* **11** (1975) 963.
8. L. V. NEWMANN and J. G. WILLIAMS, *Polym. Eng. Sci.* **20** (1980) 572.
9. O. F. YAP, Y. W. MAI and B. COTTERELL, *J. Mater. Sci.* **18** (1983) 657.
10. I. M. WARD, *ibid.* **6** (1971) 1397.
11. D. J. TOWNSEND and R. C. WARREN, *Polymer* in press.
12. S. VENZI, A. H. PRIEST and M. J. MAY, ASTM STP 466 (American Society for Testing and Materials, Philadelphia, 1970) p. 165.
13. O. L. DAVIES, (ed.), "Statistical Methods in Research and Production" (Oliver and Boyd, London, 1961).
14. R. F. BOYER, *Polymer* **17** (1976) 996.
15. B. HARTMANN and G. F. LEE, *J. Appl. Polym. Sci.* **23** (1979) 3639.
16. B. HARTMANN and G. F. LEE, *J. Appl. Polym. Sci.* **23** (1979) 3639.

Received 20 March
and accepted 15 October 1984